

Textile Research Journal

<http://trj.sagepub.com/>

Betelnut fibres as an alternative to glass fibres to reinforce thermoset composites: A comparative study

Umar Nirmal, Jamil Hashim, Saijod TW Lau, Yuhazri My and BF Yousif
Textile Research Journal 2012 82: 1107 originally published online 7 March 2012
DOI: 10.1177/0040517512439945

The online version of this article can be found at:
<http://trj.sagepub.com/content/82/11/1107>

Published by:



<http://www.sagepublications.com>

Additional services and information for *Textile Research Journal* can be found at:

Email Alerts: <http://trj.sagepub.com/cgi/alerts>

Subscriptions: <http://trj.sagepub.com/subscriptions>

Reprints: <http://www.sagepub.com/journalsReprints.nav>

Permissions: <http://www.sagepub.com/journalsPermissions.nav>

Citations: <http://trj.sagepub.com/content/82/11/1107.refs.html>

>> [Version of Record](#) - Apr 24, 2012

[OnlineFirst Version of Record](#) - Mar 7, 2012

[What is This?](#)

Betelnut fibres as an alternative to glass fibres to reinforce thermoset composites: A comparative study

Umar Nirmal¹, Jamil Hashim¹, Saijod TW Lau¹, Yuhazri MY²
and BF Yousif³

Textile Research Journal
82(11) 1107–1120
© The Author(s) 2012
Reprints and permissions:
sagepub.co.uk/journalsPermissions.nav
DOI: 10.1177/0040517512439945
trj.sagepub.com



Abstract

For the current work, investigations were carried out using treated betelnut fibre-reinforced polyester (T-BFRP) and chopped strand mat glass fibre-reinforced polyester (CSM-GFRP) composites. Results revealed that T-BFRP showed competitive performance of about 1.16%, 17.39% and 4.92% for tensile, flexural and compression tests as compared to the latter. Through tribological performance tests, T-BFRP composite showed superiority in wear for the dry and wet tests of about 98% and 90.8% while the friction coefficient was reduced by about 9.4% and 80% respectively. The interface temperature was lower by about 17% for T-BFRP composite subjected to dry test as compared to CSM-GFRP. SEM analysis revealed that the brittle effects observed on glass fibres during the tribo test enhanced the material removal rate which increased the thermo-mechanical effects at the rubbing zone. As such, evidence of adhesive to abrasive wear transition was observed when the CSM-GFRP composite was subjected to the stainless steel counterface. On the contrary, T-BFRP composite formed a thin layer of shield (i.e. back film transfer) on its worn surface during the test, which assisted in lowering the material removal rate.

Keywords

Natural fibre, synthetic fibre, mechanical, wear, friction, polymer-matrix composite

Introduction

Nowadays, fibre-reinforced composites are known to be the best substitutes for metals due to their structural properties and availability. Paul et al.¹ and Khan et al.² reported that synthetic fibres, namely glass and carbon fibres, are widely used as composite materials in applications such as: aerospace industries, marine sectors, in the making of sport equipments and automotive components due to their lightweight, responsive strength and rigidity characteristics. Macroscopically, producing synthetic fibres consumes a high amount of energy,^{2,3} which may lead to the contribution of greenhouse effect. Furthermore, Khan et al.² reported that synthetic fibres may cause potential health problem to human beings when dealing/processing glass fibre particulates. Interestingly, natural fibres are gaining much attention among researchers namely to explore the possibility of replacing synthetic fibres. Many researchers agreed on the advantages possessed by natural fibres

compared to synthetic fibres. Naming a few, Paul et al.,¹ Joshi et al.,³ Dillon,⁴ Yousif and El-Tayeb,⁵ and Nirmal and Yousif⁶ revealed in their work that natural fibres are fully biodegradable, low in density, high-specific strength, cheap, aplenty in availability and flexible in usage.

Over the past decade, much research work^{1,2,4,7–9} was carried out to explore the possibility of substituting glass fibres with natural fibre reinforced polymeric composites. Results from the literature reported that glass fibre composites were more superior in mechanical

¹Multimedia University, Bukit Beruang, Malaysia

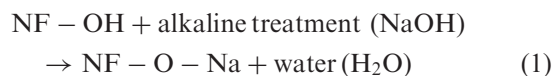
²Universiti Teknikal Malaysia, Durian Tunggal, Malaysia

³University of Southern Queensland, Australia

Corresponding author:

Umar Nirmal, Multimedia University, Jalan Ayer Keroh Lama, Bukit Beruang, 75450, Malaysia
Email: nirmal288@yahoo.com, nirmal@mmu.edu.my

properties compared to natural fibre composites. This is mainly due to the characteristics observed by glass fibres such as their hydrophobic behaviour and high fibre specific strength.^{2,10} On the contrary, Paul et al.¹ and Dillon⁴ reported that natural fibre can replace glass fibre in applications that do not need high bearing load capacity. In addition, the interest of treating natural fibres using suitable chemical solutions and coupling agents has been proven to boost the mechanical properties of its composites. Sgriccia et al.¹⁰ reported that kenaf fibre treated with a saline coupling agent is equally competitive in mechanical performance when compared to glass fibre composite. Aziz and Ansell¹¹ reported that 6% of sodium hydroxide treatment on long kenaf and hemp fibre/polyester composite showed excellent results in mechanical properties compared to glass fibre composite. Nirmal et al.¹² reported that treated betelnut fibre/polyester composites tested under adhesive dry and wet contact conditions had excellent wear performance compared to glass fibre composites. This was due to the high interfacial adhesion strength achieved between the fibre and matrix, which prevented fibre pullout during the test. In previous works conducted by Yousif and El-Tayeb,^{13,14} the interfacial adhesion of oil palm fibre was highly improved when the fibre was treated with 6% NaOH, due to the disruption of hydrogen bonding in the fibre's network structure. Nevertheless, it directly increased the surface roughness of the fibre. Similar findings were reported by Agrawal et al.,¹⁵ where they indicated that a certain amount of oil, lignin and wax covering the outer surfaces of the natural fibre have been removed due to the treatment. As a result of the treatment, it exposes the short length crystallites while depolymerizing the cellulose. On a microscopic point of view, the chemical reaction in equation 1 shows that the ionization of the hydroxyl group to alkoxide occurs on natural fibres (NF) due to the addition of NaOH.



In summary, Jähn et al.¹⁶ concluded that the alkaline treatment directly influences the extraction of lignin and the polymerization of hemicellulosic compounds and cellulosic fibril which improves surface wettability of NF against the matrix. The treatment also gave better surface roughness (i.e. removing foreign impurities and entanglements of fine hair) which improved the interlocking characteristics of the fibre and matrix. This phenomenon has been confirmed by Valadez et al.¹⁷ where it was discovered that alkaline treatment has two effects on the fibre: it increases surface roughness resulting in better mechanical interlocking and amount

of cellulose exposed on the fibre surface, thus increasing the number of possible reaction sites.

Concerning bearing applications, El-Tayeb et al.¹⁸ and Navin et al.¹⁹ reported that glass fibre-reinforced polyester (GFRP) composite tested in anti-parallel (AP) orientation with respect to the sliding direction gave high wear resistance compared to parallel (P) and normal (N) orientations. This was due to the formation of a thin layer consisting of broken fibres and fibre pullout from the fibrous region, coupled with fragmentation of polyester from the resinous region, which assisted in preventing high material removal process during longer sliding distance. El-Tayeb²⁰ reported that the chopped strand mat glass fibre-reinforced polyester (CSM-GFRP) composite has better wear resistance compared to short unidirectional sugarcane fibre/polyester composites. However, Yousif and El-Tayeb²¹ claimed that oil palm fibre-reinforced polyester (OPRP) composite under two body abrasion tests showed lower weight loss compared to CSM-GFRP composite due to the high strength of adhesion achieved between oil palm fibre and the matrix. Moreover, the authors stated that a transition from abrasive to adhesive mechanism is possible when fragments of OPRP composite are transferred onto the counterface during the 'detached-attached-detached' process.

For the current work, betelnut fibre is proposed as a potential commercial substitute to CSM glass fibre for reinforcement in polymeric composites due to a variety of reasons. For instance, betelnut fibre has a low fibre density compared to glass fibres, is fully renewable and recyclable,⁶ has lower abrasiveness to machines, is non-hazardous to health² and fully biodegradable.^{6,12} Besides that, other research,^{6,22,23} has reported that betelnut fruits are highly abundant in Malaysia. Looking at the chemical composition in betelnut fibre husks (Table 1); the fibres are composed of varying proportions of cellulose, lignin, pectin and protopectin which make them a good substitute for reinforcement purposes. For instance, Jacob et al.²⁴ and Khalil et al.²⁵ reported in their findings that the content of cellulose in certain natural fibres makes them highly hydrophilic (attracts water), which leads to more water uptake by the cell walls of the fibres surfaces and thus weakens its fibre properties (i.e. tensile strength). Conversely, betelnut fibres have certain percentage of lignin on its outer fibre surfaces making it hydrophobic, thus, preventing large amount of water absorption into the fibre core.¹⁰ Additionally, the decaying of betelnut fibre husks when composted to the soil will result in the production of nitrogen, potassium pentoxide and potassium oxide.²⁶ Ramachandra et al.²⁶ indicated in their work that these chemical substances are important to the soil as they acts as fertilizers, thus increasing the soil fertility.

Table 1. Average chemical composition (%) for betelnut fibre²³

Chemical composition	Average (%)
Cellulose	35.0–64.8
Lignin	13.0–26.0
Pectin	9.2–15.4
Nitrogen	1.0–1.1
Potassium pentoxide	0.4–0.5
Potassium oxide	1.0–1.5

Table 2. Comparison between betelnut and CSM-glass fibres

Parameters	Betelnut fibres	CSM-glass fibres
Density	0.019–0.021 g/cm ³	0.045–0.064 g/cm ^{3,18}
Cost	Highly abundant	\$1.50–\$2.00/kg ^{6,30}
Renewability	Yes	No
Recyclability	Yes	No
Energy consumption	Low	High
Distribution	Wide	Wide
CO ₂ neutral	Yes	No
Abrasion to machines	Low (fibres are soft)	Yes (fibres are hard)
Health risk	No	Yes
Disposal	Biodegradable	Non-biodegradable

The above findings are summarized in Table 2, highlighting the main difference between betelnut and CSM glass fibres. From the table, it is obvious that betelnut fibres are more favorable as compared to CSM glass fibres.

In regard to the above considerations, the authors found an interest to use betelnut vs. glass fibres as potential reinforcing elements in polymeric composites aiming to explore on the mechanical and tribological performance of these composites. Tensile, flexural, compression and hardness properties of the developed composites have been investigated based on ASTM^{27–29} standards. For the tribological tests, a developed Block-on-Disc (BOD) machine has been used to simulate the wear and friction performance of the T-BFRP and CSM-GFRP composites, subject to dry and wet contact conditions. The adhesive sliding of the composite was conducted on a smooth stainless steel counterface at a sliding velocity of 2.8 m/s, at applied loads of 30 N and 200 N, for dry and wet contact conditions. Based on the results obtained, a comparative study was performed on the potential substitution of CSM-GFRP with T-BFRP composite in relevant applications.

Material preparation

Preparation of fibres

Raw betelnut fruits (Figure 1a) are found in abundance, in particular in the state of Kedah, Malaysia. The betelnuts have to be crushed first in order to remove the seeds. The crushed betelnuts were then rinsed and soaked in water for two days to ease the fibre extraction process. While still wet, the outer layers of the betelnut fruit were removed followed by extraction of the fine fibres (Figure 1b) using a fibre extractor machine with bubbling wash effect (FEM-BWE), which was previously designed and fabricated by Nirmal.³¹ Then, the extracted fibres (Figure 1c) were treated in water containing 6% sodium hydroxide (NaOH) solution for half an hour at room temperature ($28 \pm 2^\circ\text{C}$). This was done to remove foreign substances on the fibre and to enhance the adhesion characteristics between the fibre and the matrix. The fibres were then taken out from the solution and rinsed with fresh water to remove the NaOH solution. Finally, the cleaned and treated fibres were arranged in a randomly distributed manner, pressed evenly into uniform mats (Figure 1d) and left to dry at room temperature ($28 \pm 2^\circ\text{C}$). In order to ensure effective drying of the betelnut fibres, all treated betelnut fibre mats were dried in an oven for 5 hours at 45°C . Figure 2a and b show significant differences of the betelnut fibre before and after the treatment. A very rough surface can be seen on the treated one, Figure 2b, as compared to the untreated, Figure 2a. This is due to the significant effects of the cleaned tiny hairy spots, which protrude out from the surface of an individual betelnut fibre, termed *trichomes*. They are defined as ‘epidermal hairs found on nearly all plants taking various shapes and forms’.³¹ Therefore, the presence of *trichomes*, by nature, on the outer surface of the betelnut fibre may help improve interfacial adhesion strength of the fibre (i.e. high fibre surface roughness) in the mat, against the matrix, by minimizing fibre pullout and debonding during sliding. For chopped strand mat glass fibres; Figure 2c, it was obtained from Poly Glass Fibre Manufacturing Sdn. Bhd., Malaysia.

For the purpose of preparing the fibre mats (i.e. betelnut and glass fibres), all fibre mats were cut into the dimensions of the composite fabrication mould. The corresponding SEM images showing the randomly distributed betelnut and CSM glass fibre in mat form are presented in Figure 3. Table 3 summarizes basic properties of the betelnut and CSM glass fibre mats.

Preparation of composite

Unsaturated polyester (Butanox M-60) mixed with 1.5% of methyl ethyl ketone peroxide (MEKP) as a

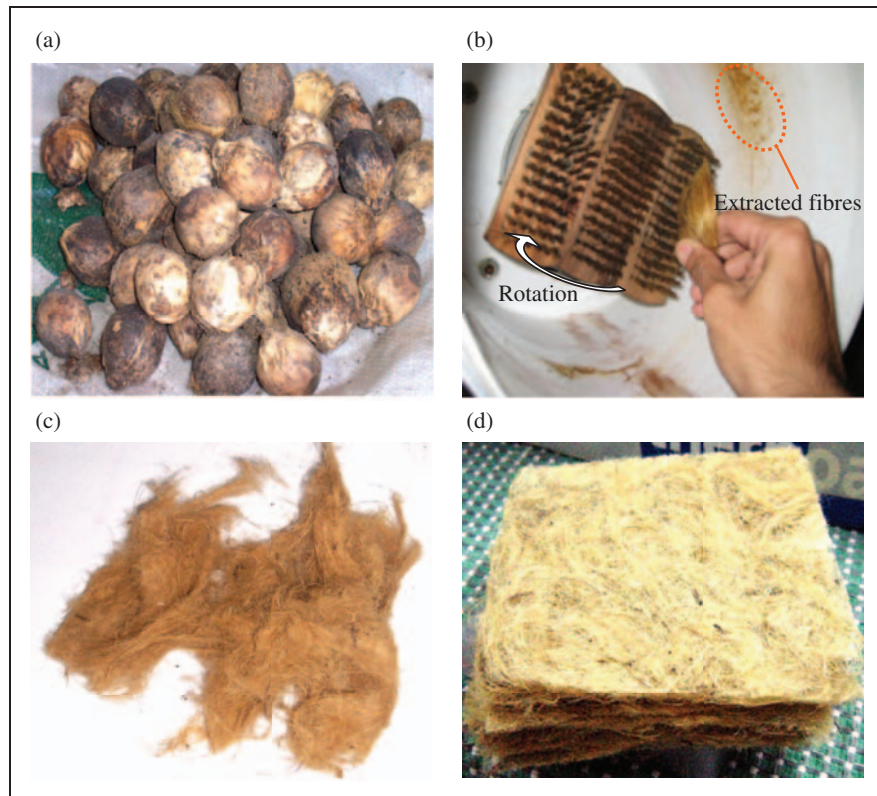


Figure 1. Steps of betelnut fibre preparation. (a) Raw betelnuts (b) Fibre extraction (c) Extracted fibre (d) Fibre mats.

catalyst was selected as a resin for the current work. Information of the resin and hardener is listed in Table 4 respectively.³²

The resin and hardener were uniformly mixed using an electrical stirrer and poured into a closed mould with a size of 100 mm × 100 mm × 10 mm. The inner surfaces of the mould were sprayed with a thin layer of silicon as a release agent. Hand lay-up technique was used, by which the first layer of the composite material was obtained by pouring the unsaturated polyester (mixed with 1.5 wt% hardener) into the mould. Subsequently, a sheet of betelnut fibre mat was placed on the first layer of polyester. A steel roller was used to even out the fibre mat and to release air bubbles from the mixture. This procedure was repeated until a maximum thickness of 10 mm was achieved (resulting with 13 layers of fibre mats and 14 layers of polyester resin). Then, a thin steel plate of the same size as the mould was placed on top of the mould's opening, pressing the composite. A pressure of about 5 kPa was applied on the steel plate to ensure that the trapped air bubbles in the composite were completely forced out. With the pressure still being applied on the mould, the composite block was left to cure for 24 hours at room temperature ($28 \pm 2^\circ\text{C}$). For thoroughness in curing, the hardened composite was removed from the mould and post-cured in an oven at 80°C for one hour. Similarly, the

CSM-GFRP composite block was fabricated using the steps explained above.

For the purpose of conducting the mechanical tests, the cured composite blocks (i.e. T-BFRP and CSM-GFRP composites) were machined into the required sizes of test samples (i.e. tensile, flexural and compression samples). Figure 4 shows the dimensions of the prepared samples according to ASTM standards.^{27–29}

For tribological tests, the test specimens with dimensions of 10 mm × 10 mm × 20 mm were prepared from the cured composite block using a Black and Decker jigsaw (Model: CD301-B1). SEM images of the virgin cross section of T-BFRP and CSM-GFRP composite test specimen are displayed in Figure 5a and b. From the figures, the approximate thickness of the polyester layer is about $130 \pm 15 \mu\text{m}$. A schematic view of the tribological test specimen showing its orientation of fibre mats with respect to the sliding direction is displayed in Figure 5c.

Experimental procedure

Mechanical test

Tensile, flexural and compression tests were conducted using a WP300 PC Aided Universal Material Test machine at room temperature ($28 \pm 2^\circ\text{C}$). Moreover, a

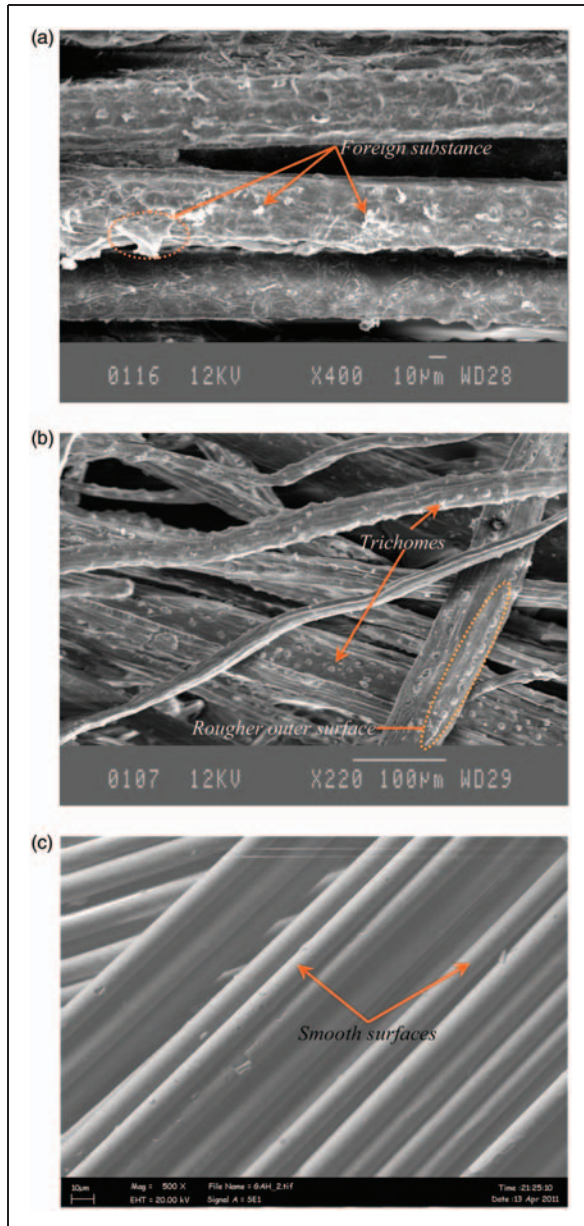


Figure 2. Micrographs of glass fibres, untreated and treated betelnut fibres. (a) Untreated betelnut fibres (b) Treated betelnut fibres (c) Glass fibres.

hardness tester (Model: TH210 ShoreD durometer) was also used to determine the ShoreD hardness of the composites. The hardness was measured perpendicular to the fibre orientation of the polyester composite (perpendicular to the thickness of 10 mm for the compression test specimen, Figure 4c).

Tribological test

A BOD machine subjected to dry and wet contact conditions was used for the current work. Water (hardness: 120–130 mg/L) was supplied to the counterface by a

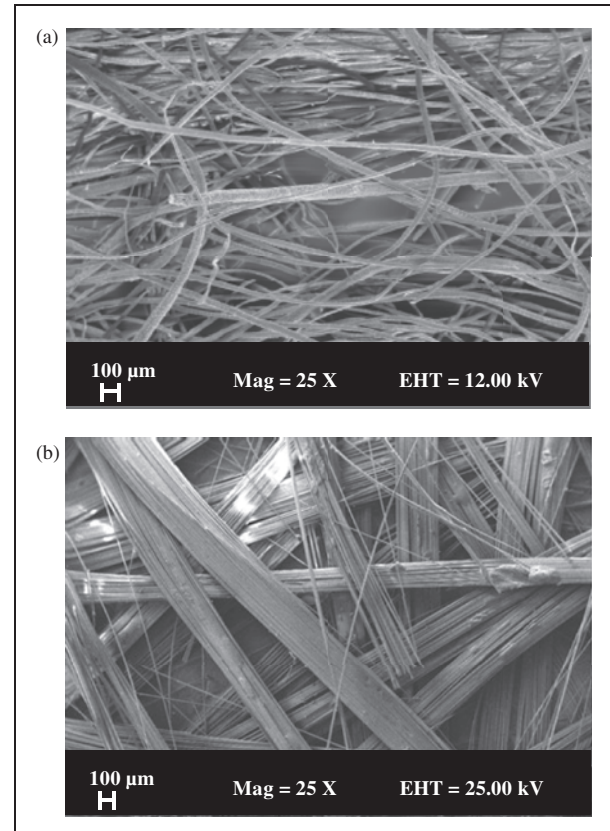


Figure 3. SEM images showing randomly distributed betelnut and CSM glass fibre in mat form. (a) Betelnut fibre mat (b) CSM glass fibre mat.

pump at a flow rate of 0.4 L/min. Water flowing off the counterface was contained by a container, with a filter being placed along the flow of water. It was cleaned from the generated wear debris after each test. An Accutec B6N-50 load cell was incorporated in the BOD load lever in order to measure the frictional forces between the specimen and the counterface. The load cell was connected to a digital weight indicator (Model: Dibal VD-310) in order to capture the frictional forces during the test. For measuring the interface temperature (i.e. temperature between test specimen and counterface), a thermocouple (Model: Center 306) was adopted where the thermocouple probe was placed at the test specimen contacting area with the counterface. Accordingly, temperature measurements were recorded for every one minute of time interval for all dry and wet testing conditions.

In a similar work done by Tong et al.,³³ subject to dry contact conditions, a higher PV limit of polyester of 1.61 MPa m/s was achieved. Accordingly, for the current work, the PV limit achieved was between 0.14–0.84 MPa m/s (equivalent to 30 N applied load at 2.8 m/s sliding velocity) for the dry conditions. It is to be noted here that 30 N of applied normal load was

Table 3. Basic properties of betelnut and CSM glass fibres

Parameters	Betelnut fibres	CSM glass fibres
Thickness of the mat	150–180 μm	160–200 μm
Length of individual fibres in mat	20–50 mm	10–60 mm
Range of the fibre diameters in mat	100 μm –200 μm	50 μm –100 μm
Density of fibre mat	200 \pm 10 g/m^2	450 g/m^2
Average distance of fibres in the mat	83 \pm 5 μm	60 \pm 5 μm
Size of the mat	100 mm \times 100 mm	
Orientation of fibres in the mat	Randomly distributed	
Fibre loading	48 vol.%	

Table 4. Specifications of the resin and hardener³²

Resin	Unsaturated polyester Butanox M-60
Colour	Colourless
Density	1370 kg/m^3 (20°C)
Hardness	84 \pm 2 ShoreD
Hardener	Methyl ethyl ketone peroxide (MEKP)
Colour	Colourless
Density	1170 kg/m^3 (20°C)
Specific gravity	1.05–1.06 (20°C)
Percentage used	1.25% (wt)

chosen for comparing the wear performance of the developed composites, since at this load there were obvious differences in the values of W_s . At a lower range of applied loads (i.e. 5–10 N), W_s was not that significant for comparison. At higher loads (>30 N), the composite failed due to the high thermo-mechanical loading incurred by the test specimens during the adhesive dry sliding test. On the other hand, under wet contact conditions, the weight loss could not be determined at low applied load (30 N) due to the low weight loss (less than 0.1 mg). Therefore, the wet tests were conducted at higher applied loads of 200 N at 2.8 m/s sliding velocity. The tests were performed at different sliding distances (0–6.72 km). The critical load was 200 N for the wet test due to the limitation of the load cell as confirmed by the supplier of the load cell, i.e. maximum loading capacity of the load cell \leq 20 kg.

Before each test, the composite test specimen was loaded into the specimen holder and abrasive paper of grade 800 was placed between the counterface and the test specimen. With a normal load of 20 N applied, the counterface was turned manually to achieve sufficient intimate contact. This procedure was repeated on the same test specimen but with a different abrasive paper of grade 1000. This was to minimize mechanical interlocking of the specimen against the counterface during testing. Upon completion, the test specimen

was taken out, cleaned with a wet cloth, dried and weighed using a weighing scale (Model: Setra weight balance, \pm 0.1 mg) before the experiment.

Concerning the stainless steel counterface, it was polished with abrasive papers starting with grade 200, 500, 1000 followed by 2000. After polishing, the counterface was cleaned with liquid acetone by means of a clean cloth. To avoid conflict in friction readings generated during the test which might be influenced from any thin layer of acetone remaining behind during the counterface cleaning process, the whole counterface was wiped with a wet cloth and dried at room temperature ($28 \pm 2^\circ\text{C}$) before each test. This procedure was repeated for all dry and wet tests. For the wet tests, all specimens were dried in an oven at a temperature of 40°C for 24 hours. The specific wear rate was computed using equation 2. The weight losses of the specimen were determined using a Setra weight balance (\pm 0.1 mg).

$$W_s = \frac{\Delta V}{F_N \cdot D} \quad (2)$$

where W_s = specific wear rate (mm^3/Nm); ΔV = volume difference (mm^3); F_N = normal applied load (N); D = sliding distance (m)

Results and discussions

As a result of repeating the mechanical and tribological experiments three times, the standard deviation is computed which is presented in Figure 6.

It is to be highlighted here that, due to the nature of the betelnut fibre husks being fine and short, it was impossible for a uni-directional or bi-directional layout. Thus, randomly distributed fibres were preferred during composite fabrication. For comparing purposes and on the prospect of potential substitution in mechanical and tribological applications of polymeric composites, CSM glass fibre was used as a

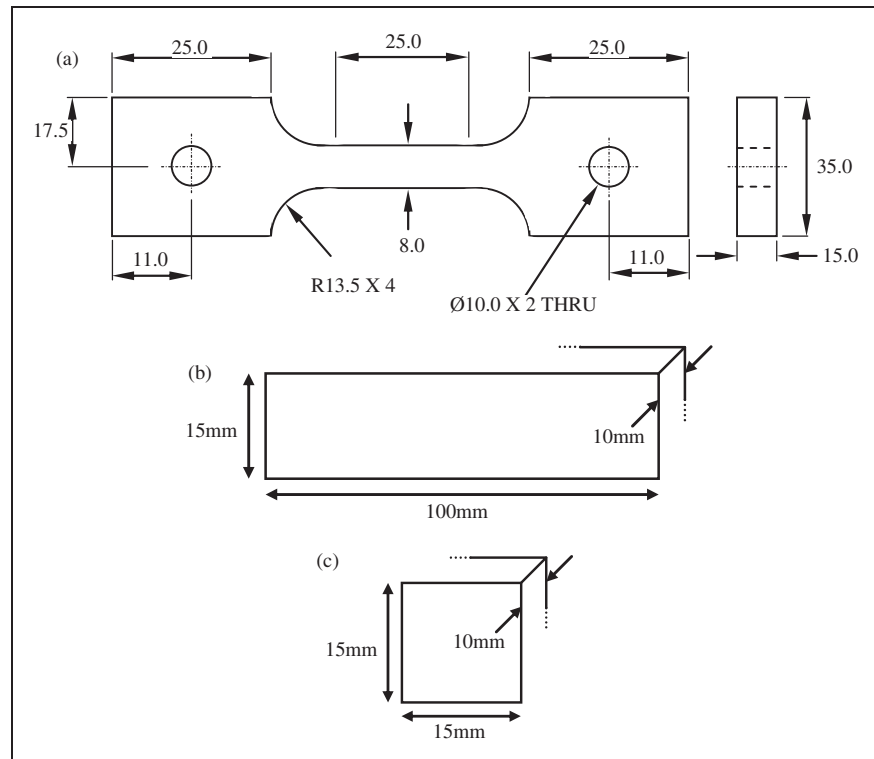


Figure 4. Schematic illustration of different test specimens for conducting the mechanical test. (a) Tensile test specimen²⁴ (b) Flexural test specimen²⁵ (c) Compression and hardness test specimen.²⁶

comparison since it possesses close or similar characteristics to betelnut fibres (i.e. randomly distributed).

Mechanical performance of T-BFRP vs. CSM-GFRP composites

Mechanical performance of the T-BFRP and CSM-GFRP composites are presented in Figure 7. A visual examination of Figure 7a reveals different trends of mechanical properties for the two types of composites, (i.e. T-BFRP vs. CSM-GFRP). It can be seen that the T-BFRP composite exhibits competitive performance in tensile, flexural and compression strength compared to the CSM-GFRP composite. From the figure, the T-BFRP composite showed up to 1.16%, 17.39% and 4.92% in variation for tensile, flexural and compression tests compared to the latter.

With a fibre to resin ratio of about 48%, by volume, used during composite fabrication for both betelnut and CSM glass fibres, the T-BFRP composite has a hardness of about 8.54% higher, compared to CSM-GFRP (Figure 7b). Thus, as suggested by Tsukada et al.³⁴ and Hariharan et al.,³⁵ T-BFRP composite can be made applicable to applications where hardness is of an important factor, such as in the making of partition boards, doors, window panels and ceilings.

Though betelnut fibre mechanical properties (i.e. tensile, flexural and compression) are lower than those of glass fibres, their specific properties, especially fibre stiffness, are comparable to the stated values of glass fibres. Figure 8 shows a typical average load-displacement diagram for the glass and treated betelnut fibre through single fibre pullout test (SFPT). The figure indicates that the betelnut fibre exhibits ductile-like behaviour during the test where the maximum pullout force was about 16 N at a fibre elongation of approximately 4 mm. However, glass fibre exhibits a maximum pullout force of about 17 N at a shorter fibre elongation of about 1.5 mm, (i.e. brittle behaviour).

Tribological performance of T-BFRP vs. CSM-GFRP composites

The wear and frictional performance of the T-BFRP and CSM-GFRP composites at dry and wet contact conditions are presented in Figure 9a and b. T-BFRP composite showed superiority in wear of about 98% for dry and 90.8% for wet tests, while the friction was lower by about 9.4% and 80% for the dry and wet tests compared to CSM-GFRP. These significant improvements in wear and friction property propose

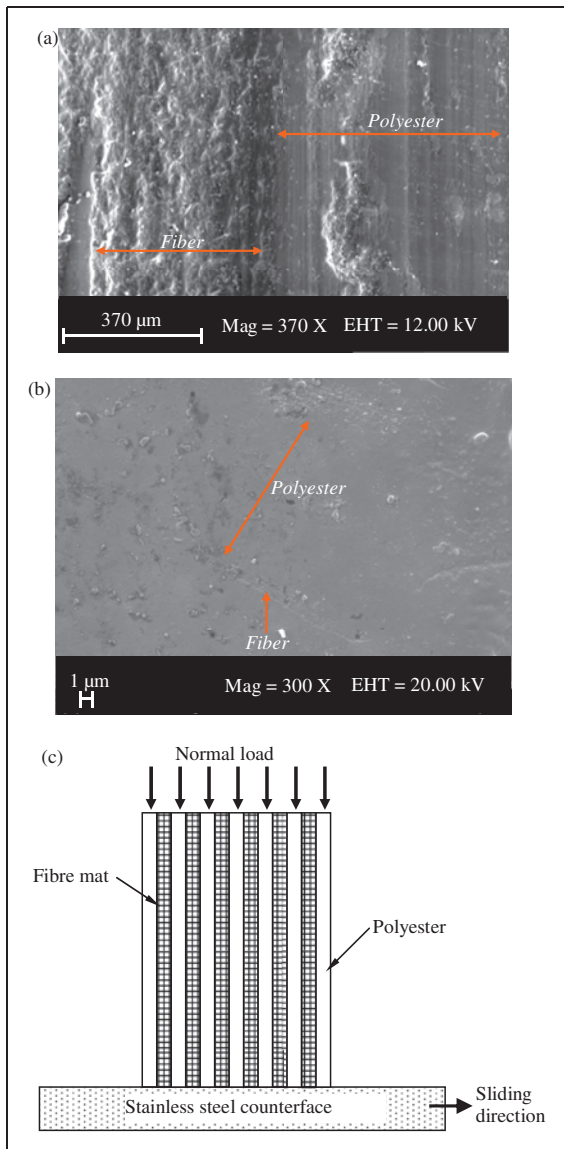


Figure 5. SEM of the virgin test specimens and corresponding schematic illustration of the specimen showing fibre orientation and sliding direction. (a) Virgin surface of the T-BFRP composite test specimen (b) Virgin surface of the CSM-GFRP composite test (c) Schematic illustration of T-BFRP composite showing fibre mats orientation with respect to the sliding direction.

the T-BFRP composite to be a potential candidate to substitute the latter concerning applications related to tribology. Further analysis on the worn surfaces of the composites will be discussed below with the assistance of SEM images.

Temperature performance of T-BFRP vs. CSM-GFRP composites

The temperature performance for T-BFRP and CSM-GFRP composites under dry and wet contact

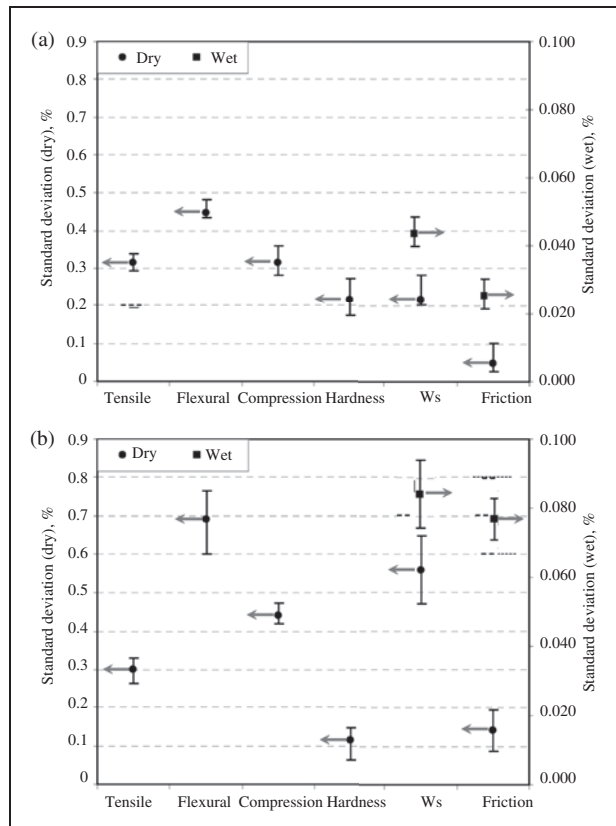


Figure 6. Corresponding standard deviation for the different types of composites. (a) T-BFRP (b) CSM-GFRP.

conditions are presented in Figure 10. Figure 10a shows the temperature profiles of the two different composites at different sliding distances. The measurements were taken at every one minute of time interval for a total sliding distance of 6.72 km throughout the dry and wet tribological tests.

From Figure 10a, it can be seen that there is a gradual increment between the interface temperature (<4.5 km) for both composites subjected to dry contact condition. This is due to the effect of thermo-mechanical loading evidenced during adhesive dry sliding. At longer sliding distance (>4.5 km), the temperature rise was more significant due to the fact that there was severe plastic deformation by the composites. Hence, the resinous regions were easily deformed thereby lowering the adhesion of fibres/matrix which enhanced the material removal process. Further examination of the composite worn surfaces will be discussed as below with the assistance of SEM images. When the composites were subjected to wet contact conditions, the effect of thermo-mechanical loading was completely eliminated when water was supplied to the interfaces (i.e. test specimen and counterface). Thus, the interface temperature of the T-BFRP and CSM-GFRP composite test specimens was constant throughout the test,

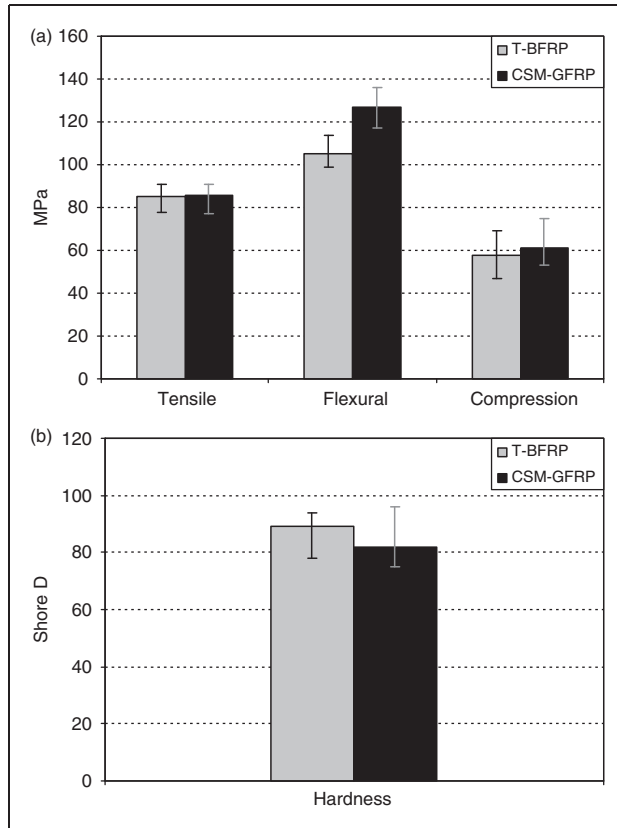


Figure 7. Mechanical performance of T-BFRP and CSM-GFRP composites. (a) Mechanical properties (b) Hardness properties (c) Hardness.

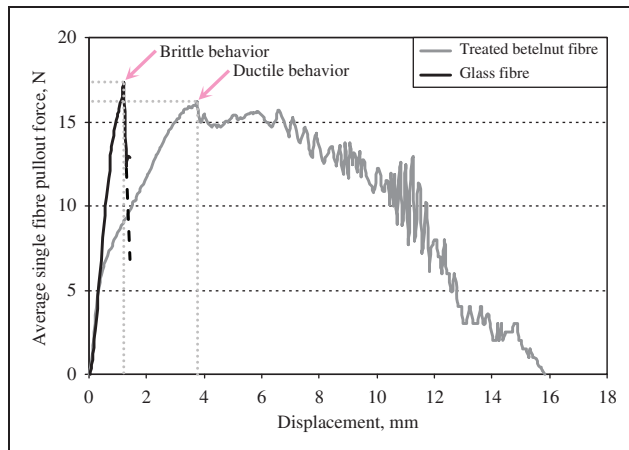


Figure 8. SFPT for glass and treated betelnut fibre.

which is confirmed by the temperature profiles in Figure 10a. The effect of different fibre reinforcements in polyester composites on average interface temperatures is presented in Figure 10b. From the figure, reinforcing polyester with betelnut fibres has lowered the interface temperature by about 17% compared to glass fibres under a dry adhesive test. The interface

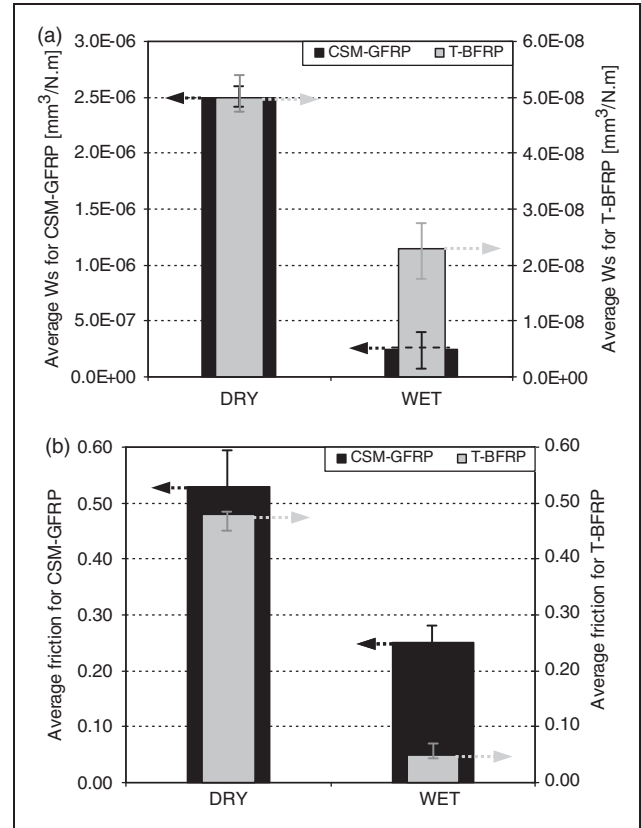


Figure 9. Tribological performance of T-BFRP and CSM-GFRP composites. (a) Specific wear rate (b) Friction coefficient.

temperature for CSM-GFRP composite was high due to the brittle effects of glass fibres which could influence the transition of wear mechanism from adhesive to abrasive between the interacting zones (i.e. test specimen and counterface). In the case of wet contact condition, supplied water at the interfaces kept the interacting surfaces clean from generated wear debris while maintaining the contact temperature constant throughout the test.

To further clarify the results, Figure 11 is presented where it explains the possible wear mechanism that took place during the adhesive wear test subjected to dry and wet contact conditions for the T-BFRP and CSM-GFRP composites. From Figure 11a, when the composite test specimen (soft) is in contact with the stainless steel counterface (hard), three contact mechanism may have taken place. They are known as 'cold welding' and 'rupture' due to the uneven surface of the test specimen. Besides that, fine wear particles that cannot be detected by the naked eyes may have also been present between the interfaces. When the sliding starts, rupture of the uneven surface from the test specimen takes place causing a third body between the interfaces. This third body (from the resinous or fibrous region) with the trapped wear particles might have been

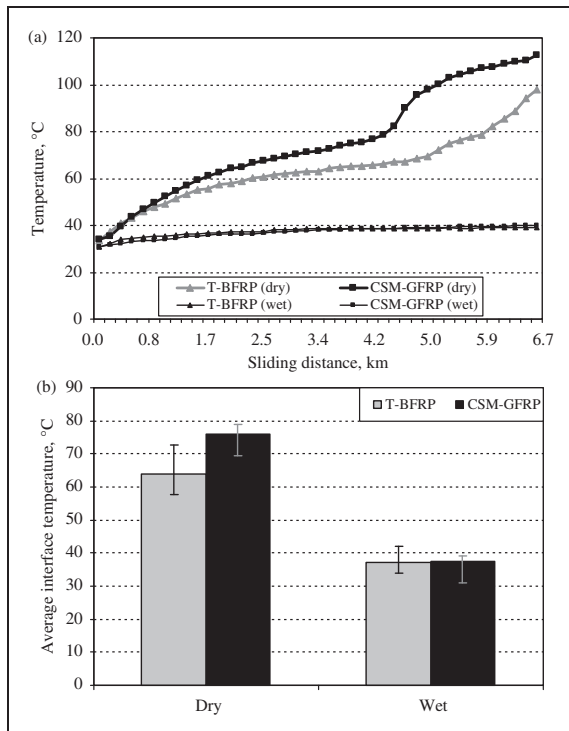


Figure 10. Temperature performance of the T-BFRP and CSM-GFRP composites at dry and wet conditions. (a) Temperature profiles of the composites (b) Average interface temperature of the composites.

in circular or linear motion between the interfaces during the adhesive dry sliding causing film transfer onto the counterface. Therefore, a possible wear mechanism on the top surface of the film transfer could be 'galling' (due to the circular motion of wear debris between the interfaces) or 'scoring' (due to linear motion of wear debris between the interfaces). This can cause high resistance of relative motion during the adhesive dry test and thus contributing to a much higher interfaces temperature.

On the contrary, Figure 11b illustrates a different sliding mechanism for the wet test during start up. From the figure, the gap formed between the composite test specimen and the counterface, due to the formation of 'cold welding' and trapped wear particles, is now filled with water. It is also to be highlighted here that water was introduced to the counterface before the adhesive wet test was carried out. Hence, during the test, deformation of 'cold welding' and rupture of the uneven joints of the composite test specimen were instantly washed away from the interfaces with the help of clean flowing water. This eliminates the presence of a third body (from the resinous or fibrous region) and the formation of film transfer at the interface. Thus, the ease of relative motion due to the presence of water contributes to a drastic drop in static to kinetic friction

coefficient. Besides, thermo-mechanical loading is also eliminated since water had also played a role to keep the counterface temperature constant throughout the test.

Morphology of the worn surfaces through SEM analysis

Surface morphology of the samples was analyzed through SEM (model: EVO 50 ZEISS-7636). Before taking the SEM images, the samples were coated with a thin layer of gold using ion sputtering (model: JEOL, JFC-1600). All observing conditions were performed at room temperature of $28 \pm 5^\circ\text{C}$ and at humidity level of $80 \pm 10\%$.

The worn surfaces for the different composites subjected to dry contact condition at $1000\times$ magnification are presented in Figure 12. Different wear features are evidenced on the worn surfaces subjected to different fibre reinforcements in polyester composites. An obvious sign of plastic deformation can be observed at the resinous regions for the T-BFRP composite, associated with sign of softened polyester (Figure 12a). This is due to the high intimate contact of the test specimen and counterface causing the polyester to melt with the influence of severe thermo-mechanical loading at longer sliding distances (i.e. 6.72 km). In regard to this, part of the fibres received poor support from the polyester matrix, which contributed to the high material removal rate (i.e. from the fibrous regions). This is confirmed with the sign of fine debris evidenced on the worn surface. Also, there were signs of embedded fibres in the matrix on the worn surface, Figure 12a. This could be due to the effects of *trichomes* on the betelnut fibre surfaces which assisted to lock the fibres firmly in the matrix preventing complete fibre pullout.

On the contrary, the wear damage was much more significant when CSM-GFRP composite was subjected to the counterface (Figure 12b). It can be seen that the glass fibre was deformed at longer sliding distance (i.e. 6.72 km). Besides that, there was also sign of fractured and deformed polyester at the resinous regions. This further caused damage onto the glass fibre (i.e. the fibre was easily broken apart due to the excessive sliding shear force by the worn polyester debris). Arguably, the combined brittle nature of worn polyester debris and glass fibres led to the formation of fine/coarse abrasive wear particles as evidenced in Figure 12b. This further reduced the wear performance of the composite, namely when these particles interacted at the contacting zones by enhancing the material removal rate by a factor of $99 \times 10^{-8} \text{ mm}^3/\text{Nm}$ compared to the T-BFRP composite (Figure 10a). Moreover, loose abrasive particles and polyester debris at the rubbing zone assisted to increase the friction coefficient and

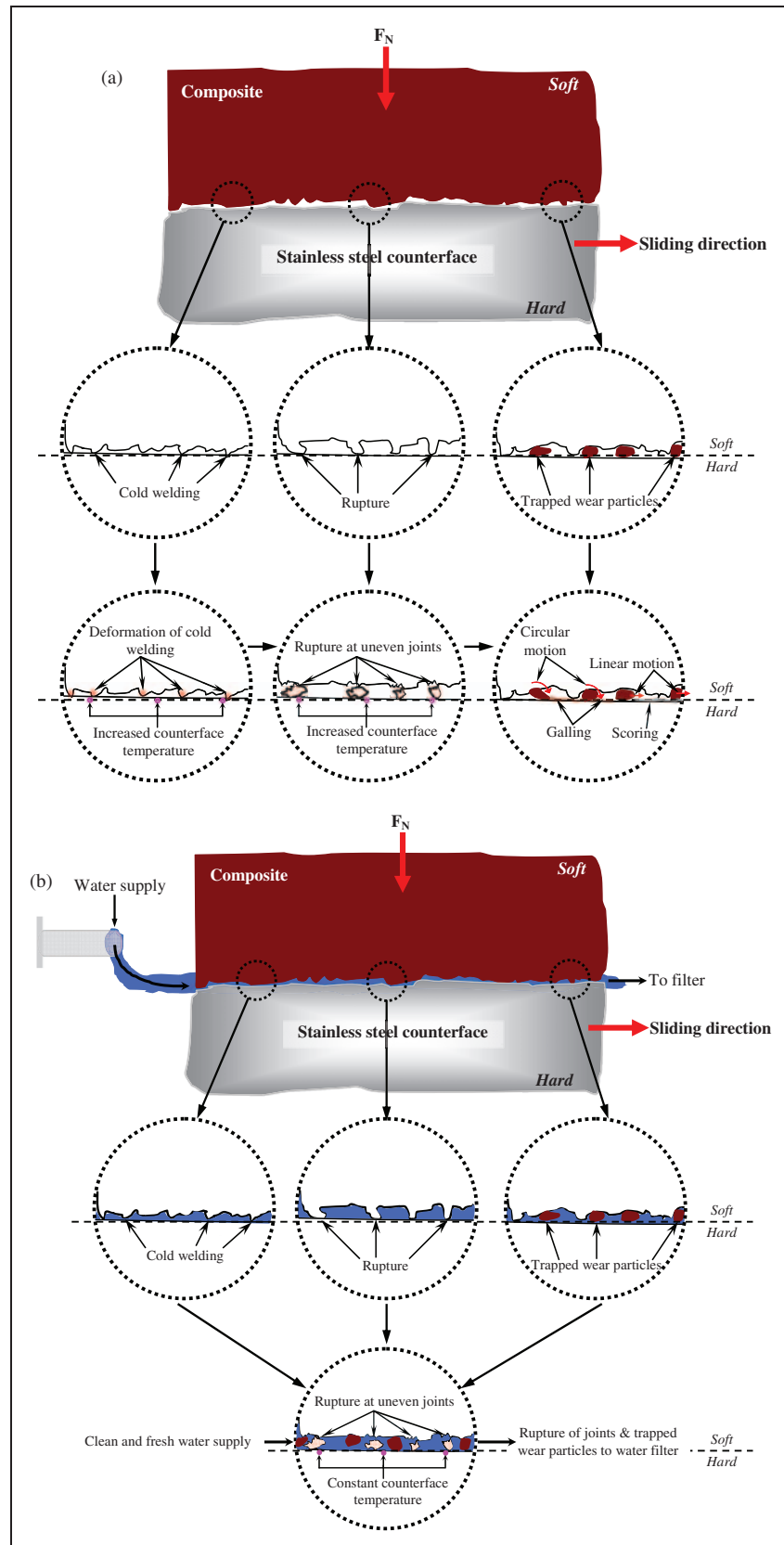


Figure 11. Adhesive sliding mechanism for dry and wet contact conditions. (a) Sliding mechanism for adhesive dry test (b) Sliding mechanism for adhesive wet test.

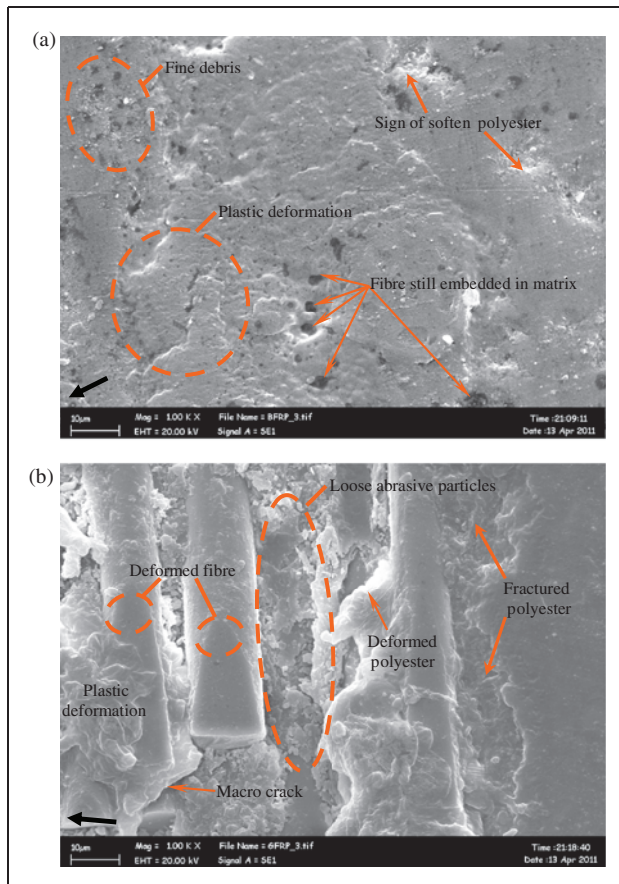


Figure 12. SEM images of the T-BFRP and CSM-GFRP composites at dry contact condition subjected to an applied load of 30 N, 6.72 km sliding distance and 2.8 m/s of counterface sliding velocity. (a) T-BFRP (b) CSM-GFRP.

interfaces temperature which is confirmed by Figure 9b and Figure 10.

Due to the fact that T-BFRP composite revealed less damage than the CSM-GFRP composite, the possible suggestion of the proposed T-BFRP composite can be in non-structural applications^{1,4} since many attempts have been made to use natural fibre composites in place of glass fibre composites. In addition to this, Dahlke et al.,³⁶ Quig et al.,³⁷ Fukuhara³⁸ and Leao et al.³⁹ reported that a good number of automotive components previously made with glass fibre composites are now being manufactured using environmentally friendly composites. Moreover, Eberle and Franze⁴⁰ further claimed that automotive giants, such as Daimler Chrysler and Mercedes Benz, are continuously producing low weight vehicles, in recent years, using large amounts of renewable fibres in composite fabrication, since for every 1 kg of weight reduction of an automobile vehicle, as much as 5.95 to 8.4 L of petrol can be saved. Secondly, as suggested by Bhushan⁴¹ and Cirino et al.,⁴² the proposed T-BFRP composite can be used as bearing and sliding materials, subjected to

tribological loading conditions due to their low friction conditions (i.e. wet conditions), high wear resistance and easy process ability properties.

Though T-BFRP composite offer several benefits as compared to CSM-GFRP composite, several major technical considerations must be addressed before the engineering, scientific and commercial communities gain the confidence to enable wide-scale acceptance, particularly in exterior parts where a Class A surface finish is required. To name but a few, these challenges include in-depth investigation on the homogenization of the fibre properties and a full understanding of the degree of polymerization and crystallization, adhesion between the fibre and matrix, moisture repellence, and flame retardant properties.

Conclusions

Based on the results obtained, the following conclusions are drawn:

1. Betelnut fibres have commercial benefits. This may be attributed to the surface roughness of the *trichomes* which enhance the interlocking of the betelnut fibre in the matrix and the peculiar property of the betelnut fibrous region itself.
2. In mechanical properties, T-BFRP composite was found to have equivalent tensile and compression strengths while flexural strength was lower by about 15% compared to CSM-GFRP composite. The hardness test for the T-BFRP composite was 10% superior compared to CSM-GFRP composite.
3. In tribological properties, the specific wear rate for T-BFRP composite was low by about 98% and 90.8% in both dry and wet tests compared to CSM-GFRP composite. Meanwhile the friction coefficient for T-BFRP composite was reduced by about 9.4% and 80% for the dry and wet tests as compared to the latter. Interface temperature of the T-BFRP composite was 17% lower for the dry test as compared to the CSM-GFRP composite. Under wet contact conditions, neither composites showed any significant effects of interface temperature.

Acknowledgements

The authors would like to thank Chan Wai Ti for his kind support and help contributed towards the implementation of this research.

Funding

This research received no specific grant from any funding agency in the public, commercial, or not-for-profit sectors.

References

- Paul W, Jan I and Ignaas V. Natural fibres: can they replace glass in fibre reinforced plastics? *Comp Sci Technol* 2003; 63: 1259–1264.
- Khan RA, Khan MA, Zaman HU, et al. Comparative studies of mechanical and interfacial properties between jute and E-glass fibre reinforced polypropylene composites. *J Reinforced Plast Comp* 2010; 29: 1078–1088.
- Joshi SV, Drzal LT, Mohanty AK, et al. Are natural fibre composites environmentally superior to glass fibre reinforced composites? *Comp Part A: Appl Sci Manufact* 2004; 35: 371–376.
- Dillon JH. Current problems and future trends in synthetic fibres. *Textile Res J*. 1953; 23: 298–312.
- Yousif BF and El-Tayeb NSM. Adhesive wear performance of T-OPRP and UT-OPRP composites. *Tribology Lett* 2008; 32: 199–208.
- Nirmal SG and Yousif BF. Wear and frictional performance of betelnut fibre-reinforced polyester composite. *Proc Inst MechEng Part J: J Eng Tribology*. 2009; 223: 183–194.
- Rodriguez E, Petricci R, Puglia D, et al. Characterization of composites based on natural and glass fibres obtained by vacuum infusion. *J Comp Mater*. 2005; 39: 265–282.
- Shubhra QTH, Alam AKMM and Beg MDH. Mechanical and degradation characteristics of natural silk fibre reinforced gelatin composites. *Mater Lett* 2011; 65: 333–336.
- Meiwei S, Hong X and Weidong Y. The fine structure of the kapok fibre. *Textile Res J*. 2010; 80: 159–165.
- Sgriccia N, Hawley MC and Misra M. Characterization of natural fibre surfaces and natural fibre composites. *Comp: Part A* 2008; 39: 1632–1637.
- Aziz SH and Ansell MP. The effect of alkalization and fibre alignment on the mechanical and thermal properties of kenaf and hemp bast fibre composites: Part 1–polyester resin matrix. *Comp Sci Technol* 2004; 64: 1219–1230.
- Nirmal U, Yousif BF, Rilling D, et al. Effect of betelnut fibres treatment and contact conditions on adhesive wear and frictional performance of polyester composites. *Wear* 2010; 268: 1354–1370.
- Yousif BF and El-Tayeb NSM. High-stress three-body abrasive wear of treated and untreated oil palm fibre-reinforced polyester composites. *Proc Inst Mech Eng Part J: J Eng Tribol* 2008; 222: 637–646.
- Yousif BF and El-Tayeb NSM. Wet adhesive wear characteristics of untreated oil palm fibre-reinforced polyester and treated oil palm fibre-reinforced polyester composites using the pin-on-disc and block-on-ring techniques. *Proc Inst Mech Eng Part J: J Eng Tribol* 2010; 224: 123–131.
- Agrawal R, Saxena NS, Sharma KB, et al. Activation energy and crystallization kinetics of untreated and treated oil palm fibre reinforced phenol formaldehyde composites. *Mater Sci Eng A*. 2000; 277: 77–82.
- Jähn A, Schröder MW, Fütting M, et al. Characterization of alkali treated flax fibres by means of FT Raman spectroscopy and environmental scanning electron microscopy. *Spectrochim Acta Part A: Mol Biomol Spectro* 2002; 58: 2271–2279.
- Valadez GA, Cervantes UJM, Olayo R and Herrera FPJ. Effect of fibre surface treatment on the fibre-matrix bond strength of natural fibre reinforced composites. *Comp Part B: Eng* 1999; 30: 309–320.
- El-Tayeb NSM, Yousif BF and Yap TC. Tribological studies of polyester reinforced with CSM 450-R-glass fibre sliding against smooth stainless steel counterface. *Wear* 2006; 261: 443–452.
- Navin C, Ajay N and Somit N. Three-body abrasive wear of short glass fibre polyester composite. *Wear* 2000; 242: 38–46.
- El-Tayeb NSM. Two-body abrasive behaviour of untreated SC and R-G fibres polyester composites. *Wear*. 2009; 266: 220–232.
- Yousif BF and El-Tayeb NSM. Mechanical and wear properties of oil palm and glass fibres reinforced polyester composites. *Int J Precision Eng* 2009; 1: 213–222.
- Nirmal U, Singh N, Hashim J, et al. On the effect of different polymer matrix and fibre treatment on single fibre pullout test using betelnut fibres. *Mater Des* 2011; 32: 2717–2726.
- Nirmal U. *Betelnut fibres as bio-reinforcements in polyester composites for mechanical and tribological applications*. M. Eng. Sci, Multimedia University, Malacca, 2011, p.142.
- Jacob M, Varughese KT and Thomas S. Water sorption studies of hybrid biofibre-reinforced natural rubber biocomposites. *Biomacromolecules* 2005; 6: 2969–2979.
- Khalil HPSA, Ismail H, Rozman HD, et al. The effect of acetylation on interfacial shear strength between plant fibres and various matrices. *Eur Polym J*. 2001; 37: 1037–1045.
- Ramachandra TV, Kamakshi G and Shruthi BV. Bioresource status in Karnataka. *Renewable Sustainable Energy Rev* 2004; 8: 1–47.
- ASTM D790. Standard test method flexural properties of unreinforced and reinforced plastics and electrical insulating materials.
- ASTM D695. Standard test method for compressive properties of rigid plastics.
- ASTM D638. Standard test method for tensile properties of plastics.
- Foulk J, Akin D and Dodd R. New low cost flax fibres for composites. *SAE World Congress*. Detroit, MI, USA, 2000.
- Nirmal SG. *An investigation of wear and frictional performance of betelnut fibre reinforced polyester composite under dry contact condition*. Degree Thesis, Multimedia University, Malacca, 2008, p.100.
- Akzo Nobel Polymer Chemicals. SAFETY DATA SHEET According to Regulation (EC) No. 1907/2006 BUTANOX M-60 [http://www.yucelkompozit.com.tr/images2/File/MSDS_PRD_BUTANOX%20M-60%20\(English\).pdf](http://www.yucelkompozit.com.tr/images2/File/MSDS_PRD_BUTANOX%20M-60%20(English).pdf) (2006, accessed 12 December 2011).
- Tong J, Ma Y, Chen D, et al. Effects of vascular fibre content on abrasive wear of bamboo. *Wear*. 2005; 259: 78–83.
- Tsukada M, Md. Majibur Rahman K, Tanaka T, et al. Thermal characteristics and physical properties of silk

- fabrics grafted with phosphorous flame retardant agents. *Textile Res J* 2011; 81: 1541–1548.
35. Hariharan ABA and Khalil HPSA. Lignocellulose-based hybrid bilayer laminate composite: Part I–Studies on tensile and impact behavior of oil palm fibre-glass fibre-reinforced epoxy resin. *J Comp Mater* 2005; 39: 663–684.
36. Dahlke B, Larbig H, Scherzer HD, et al. Natural fibre reinforced foams based on renewable resources for automotive interior applications. *J Cellular Plast* 1998; 34: 361–379.
37. Quig JB and Dennison RW. The complementary nature of fibres from natural and from synthetic polymers. *Textile Res J* 1954; 24: 361–373.
38. Fukuhara M. Innovation in polyester fibres: from silk-like to new polyester. *Textile Res J* 1993; 63: 387–391.
39. Leao A, Rowell R and Tavares N. Applications of natural fibres in automotive industry. *Brazil–Thermoforming process*. Cairo, Egypt: Plenum Press, 1997, pp.755–760.
40. Eberle R and Franze H. Modeling the use phase of passenger cars in LCI. In: *SAE total life-cycle conference*, Graz, Austria, 1998.
41. Bhushan B. *Principles and applications of tribology*. New York: Wiley, 1999.
42. Cirino M, Friedrich K and Pipes RB. Evaluation of polymer composites for sliding and abrasive wear applications. *Composites*. 1988; 19: 383–392.